

Supplementary Materials and Methods

Human Tissues

Human liver tissue samples were obtained from patients who received surgical resection and were diagnosed by dedicated pathologists at the Eastern Hepatobiliary Surgery Hospital (Shanghai, China), with written informed consent. The patients in the first cohort (n = 120) received surgical resection from June 2009 to February 2017. The patients in the second cohort (n = 16) received surgical resection from May 2019 to September 2019. Tumorous cells and cancer-associated fibroblasts (CAF) were isolated from tumorous tissues, and hepatocytes and peri-tumoral fibroblasts (PTF) were isolated from the non-tumorous tissues of these 16 patients according to the method reported in our previous study^[1]. All of the HCC patients were treatment-naïve before receiving resection and were followed up every three months until the development of disease progression including recurrence, metastasis or death. HCC tissues with typical macroscopic features were collected from the central part of tumor nodules which were further examined with hematoxylin-eosin (H&E) staining to confirm the diagnosis. The paired adjacent nontumoral tissues without histopathologically identified tumor cells were collected from at least 5 cm away from tumor boarder. In the total of 120 HCC patients, forty of them received sorafenib treatment after surgery. According to the guideline of HCC treatment, the criteria for sorafenib treatment include 1) the development of unresectable recurrence or metastasis after surgery; 2) postoperative pathological examination suggests a high risk of recurrence and metastasis: such as the detection of portal vein tumor thrombus and microvascular invasion. The criteria of dropping out of sorafenib treatment

include intolerable side effects caused by sorafenib treatment and disease progression after sorafenib oral administration indicating treatment failure. All human experiments were approved by the Ethics Committee of the Second Military Medical University (Shanghai, China).

RNA Extraction and Real-Time PCR

Total RNA was isolated from cells or tissues following the standard Trizol (Takara) protocol. MicroRNAs expression levels were tested using Bulge-Loop™ miRNA qRT-PCR Starter Kit (RiBio). To detect the mRNA expression levels, first-strand cDNA was synthesized from total RNA using the RT Master Mix (Takara). Transcript levels were detected using SYBR Green-based real-time PCR performed by the ABI StepOne Real-time PCR Detection System (Life Technologies). Gene expression was analyzed using the $2^{-\Delta\Delta CT}$ method. The microRNA transcript was normalized against U6. The mRNA expression was normalized against β -actin. At least three independent experiments were performed using each condition. Primer sequences are listed in Supplementary Table. 1.

Cell cultures

HEK293 cells and HCC cells including PLC/PRF/5 and YY-8103 cells were maintained in Dulbecco's modified Eagle's medium supplemented with 10% fetal bovine serum (FBS). Hep3B cells were cultured in Eagle's minimum essential medium supplemented with 10% FBS and 1% non-essential amino acid. Primary human hepatocytes were obtained from Xeno Tech.

Transfection

miR-541 mimic and miR-541 inhibitor were used to overexpress or inhibit miR-541, siRNA targeting ATG2A (siATG2A) or RAB1B (siRAB1B) were used to downregulate ATG2A or RAB1B in HCC cells. All of the plasmids, siRNA, miRNA mimic, miRNA inhibitor and their controls were transfected into cells using Lipofectamine2000 (Invitrogen) according to the instruction of manufacturer. To evaluate the effects of miR-541 mimic, miR-541 inhibitor, siATG2A and siRAB1B on the malignant properties of HCC cells, 100 pmol of the indicated miRNA mimic or inhibitor and negative control, siRNA and negative control were transfected into HCC cells. To evaluate the effects of ATG2 or RAB1B on the functional miR-541 effects in HCC cells, miRNA inhibitors (50 pmol) were co-transfected with siATG2A (50 pmol) or siRAB1B (50 pmol). Twenty-four hours or forty-eight hours after transfection, the cells were used for subsequent experiments.

Cell proliferation assay, migration assay and invasion assay

Cell Counting Kit-8 (Dojinodo, Shanghai, China) was used to analyze the proliferation of HCC cells. Cells were seeded into 96-well plates with 100 μ L culture medium. The 10 μ L of CCK-8 solution was added to the cells at specific time points and cells were incubated for 1 h at 37°C. The reaction product was quantified according to the manufacturer's instructions. Colony formation assay was performed as previously described¹ with 3×10^3 PLC/PRF/5 cells or 1×10^3 YY-8103 cells transfected with miR-541 mimic or negative control in 10 cm tissue culture plates. After 14 days of culture, visible colonies were stained with Coomassie Brilliant

Blue G250 and the numbers of colonies were counted. *In vitro* migration and invasion assays were performed by placing cells into the upper chamber of the transwell (BD bioscience) without or with Matrigel under a serum-free condition. After 24h of incubation, cells remaining on the upper chamber were removed with cotton swab; cells adhering to the lower membrane were stained with 0.1% crystal violet staining solution and analyzed under an inverted microscope (Zeiss). The area of positive staining was measured using image analyses software (Image-Pro Plus 6.0, Media Cybernetics). Migration and invasion were calculated as the percentage of positive area.

Construction of adenovirus and infection

To construct the plasmid expressing miR-541, an 864-bp fragment harboring pri-miR-541 gene was sub-cloned into the pDC315 vector using the EcoRI and NheI restriction sites. Then the resultant recombinant plasmid pDC315-miR-451 and backbone plasmid were package using AdMaxTM recombinant adenovirus packaging system to produce adenovirus expressing miR-541 (Ad-miR-541). The counterpart adenovirus harboring backbone plasmid was used as a control (Ad-MAX). The Stocks of replication-defective adenovirus were stored at -80°C. HCC cells were infected with Ad-miR-541 or Ad-MAX at an optimal multiplicity of infection (MOI) and then subjected to functional analyses at fixed time points following infection as described for individual experimental conditions.

Western blot

Proteins were extracted using lysis buffer supplemented with protease inhibitor (Roche),

separated using sodium dodecylsulfate polyacrylamide gel electrophoresis (SDS-PAGE), and then transferred onto a PVDF membrane (HAHY00010, Millipore) in constant current mode. The membrane was blocked in PBST containing 5% milk for 1 h and then was incubated with the following primary antibody at 4°C overnight. After that, 1 h incubation with a secondary antibody (donkey-anti-mouse or donkey-anti-rabbit, IRDye 700 or IRDye 800, respectively), signals were quantitated using an Odyssey infrared imaging system (LI-COR) at 700 nm or 800 nm. The primary antibodies included anti-ATG2A (PD041, MBL), anti-RAB1B (SC-599, Santa Cruz), anti-LC3 (M186-3, MBL), P62 (ab56416, Abcam) and GAPDH (BSAP0063, Bioworld).

Construction of report and luciferase assay

To construct the luciferase reporter plasmid harboring ATG2A 3'UTR or *RAB1B* 3'UTR, the full length of the 3'UTR of human *ATG2A* or *RAB1B* were sub-cloned into the psiCHECK2 vector (Promega, Madison, WI, USA) using the XhoI and NotI restriction sites. All vectors were verified by sequencing. Primer sequences are listed in Supplementary Table. 3. The 3'UTRs of human ATG2A or RAB1B with mutated miR-541 binding sites were synthesized by The Beijing Genomics Institute and subcloned into the psiCHECK2 vector.

When performing luciferase assays, HEK293 cells cultured in 24-well plate were co-transfected with 100 pmol/well miR-541 mimic or negative control (NC) and 400 ng/well psiCHECK2 plasmids using 2 µl/well Lipofectamine2000 (Invitrogen). Forty-eight hours after transfection, the Renilla and firefly luciferase activities were measured by the Dual-Luciferase Reporter Assay (Promega, Madison, WI, USA) with a luminometer

(Synergy™ 4 Hybrid Microplate Reader, BioTek, USA). The luciferase score was calculated by normalizing the luciferase signal of Renilla against that of firefly. At least three independent experiments were carried out for each condition.

50% inhibitive concentration (IC₅₀) assays

Cell viability was determined using the CCK-8 (Cell Counting Kit-8; Dojinodo, Shanghai, China) assay in accordance with the manufacturer's instructions. Briefly, the cells were transferred to 96-well plates at a density of 5,000 cells / well. Then HCC cells were firstly transfected with miR-541 mimic / negative control (NC mimic), miR-541 inhibitor / NC inhibitor, siRNA targeting ATG2A (siATG2A) or si-NC and siRNA targeting RAB1B (siRAB1B) or si-NC. Twenty-four hour after transfection, cells were treated with different dose of sorafenib dissolved in serum-free medium for 24h. Then the cell viability was tested using CCK-8 by measuring the absorbance at a wavelength of 450 nm using a microplate reader. Each experiment was repeated three times. The average inhibitory concentration 50 values (IC₅₀ values) were determined.

Immunohistochemistry (IHC)

Formalin-fixed paraffin-embedded sections were deparaffinized in xylene and rehydrated in graded alcohols. Endogenous peroxidase was blocked by 3% H₂O₂ followed by antigen retrieval. Slides were incubated with primary antibodies overnight at 4 °C and incubated with a secondary antibody at room temperature for 30 min. The following primary antibodies were used: anti-Ki67 (550609, BD PharMingen), ATG2A (SC-514207, Santa Cruz), and RAB1B

(SC-599, Santa Cruz). The staining was developed using an EnVision Detection Rabbit/Mouse Kit (GK500710, GeneTech, Shanghai, China). The IHC scores of Ki-67, ATG2A and RAB1B were quantified using the Aperio Spectrum® software (Aperio Technologies, Vista, CA) with a pixel count algorithm. Briefly, the algorithm automatically calculated the mean intensity of positive (brown staining) pixels per unit and gave a positivity score (total positive pixel units / total pixel units). The staining score for each sample was thus defined as mean intensity of positive pixels per unit \times positivity.

RNAscope® in situ hybridization

In situ hybridization was performed with paraffin embedded sections using RNAscope® technique according to the manufacturer's instructions (Advanced Cell Diagnostics (ACD), Newark, CA, USA). Briefly, four micrometers thick sections were de-paraffined and treated with RNAscope H2O2 & Protease Plus reagents (ACD #322330). Probes to human pri-miR-541 (ACD #589081) were hybridized for 2 h followed by 6 amplification steps. The signal was detected with RNAscope 2.5 HD detection kit red (ACD #322360).

Statistical Analysis

All statistical analyses were performed using SPSS version 22.0 software. Data from at least three independent experiments performed in triplicates are presented as the means \pm SD, with error bars in the bar graphs representing SD. If the data were normally distributed, comparisons of data between two groups were performed using Student's *t*-tests. If the data were skewed distribution, comparisons were performed by nonparametric test with

Mann-Whitney test in unpaired data and Wilcoxon's matched pairs test in paired data. Kaplan-Meier analysis using Log-rank test was performed to compare survival probability between different groups. Chi-square test was used to evaluate if there is a statistical difference between the amount of miR-541 and the clinical and pathologic characteristics or the recurrence rate of HCC patients. Statistical tests were two-tailed and a *P* value of less than 0.05 was considered statistically significant.

Supplementary Figures

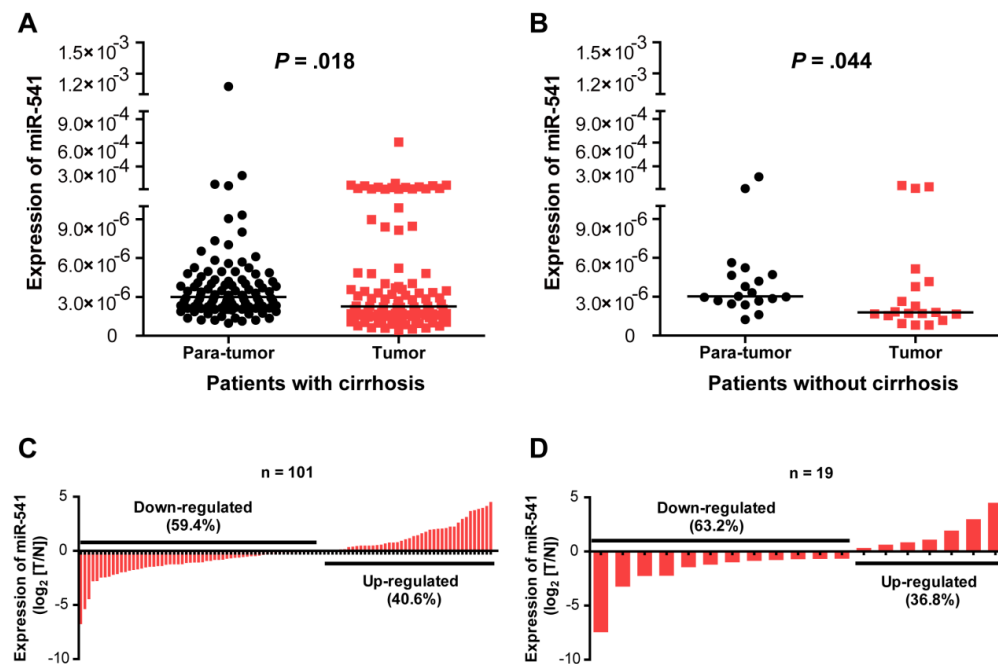


Figure S1. miR-541 was downregulated in tumorous tissues both in patients with cirrhosis and without cirrhosis.

(A and B) Statistical analysis of miR-541 expression in paired primary HCC and adjacent nontumorous liver tissues from 101 patients with cirrhosis (A) and from 19 HCC patients without cirrhosis (B), respectively. Wilcoxon matched pairs tests were used. (C and D) Real-time PCR analysis of miR-541 expression in HCCs (T) and peri-tumor normal tissues (N) from 101 patients with cirrhosis (C) and from 19 HCC patients without cirrhosis (D), respectively.

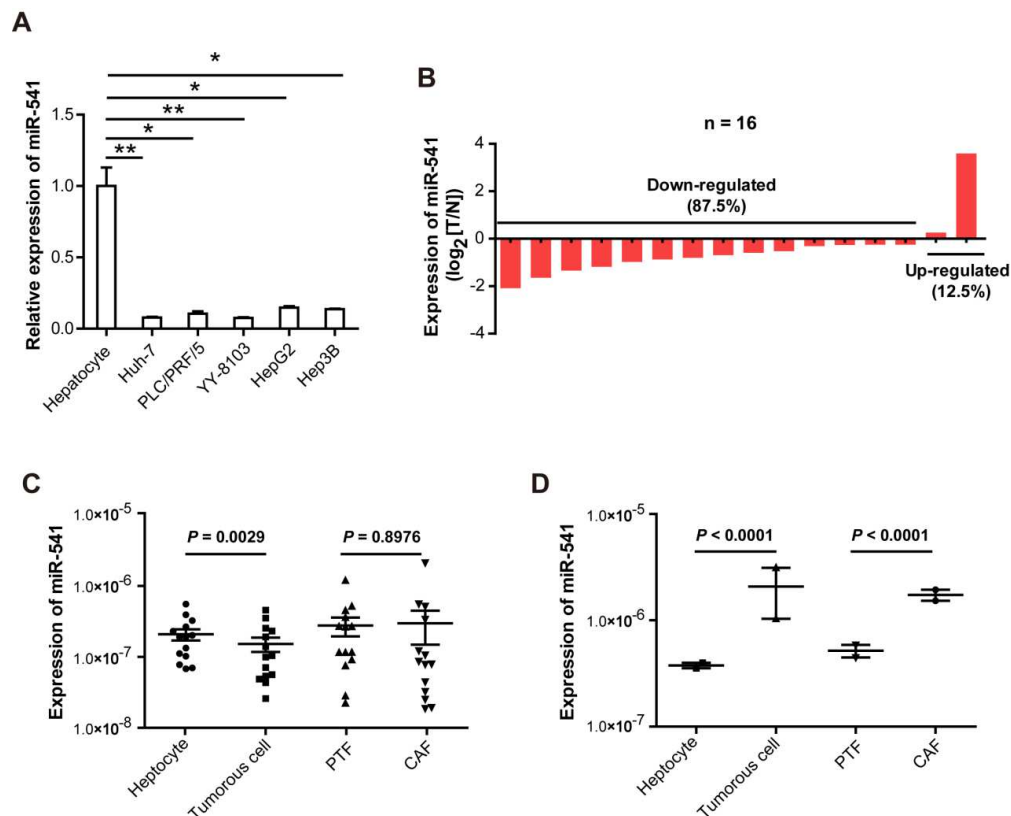


Figure S2. Expression of miR-541 was downregulated in human HCC cell lines and tissues.

(A) Primary human hepatocytes (Hepatocyte) were purchased from Xeno Tech. Real-time PCR was used to detect miR-541 expression in hepatocytes and five different HCC cell lines. Data are presented as means \pm SD. * $P < 0.05$ and ** $P < 0.01$ by two-tailed Student's t-test.

(B) Real-time PCR analysis of miR-541 expression in 16 pairs of HCCs (T) and peri-tumor normal tissues (N).

(C) miR-541 was downregulated in the tumorous cells, as compared with hepatocytes from the paired non-tumorous liver tissues in 14 patients with downregulated miR-541 in HCC. No significant difference of miR-541 levels was detected in PTF and CAF.

(D) miR-541 was increased in both of tumorous cells and CAF in 2 patients with upregulated miR-541. (C and D) Data are presented as means \pm SEM. Mann-Whitney test was used.

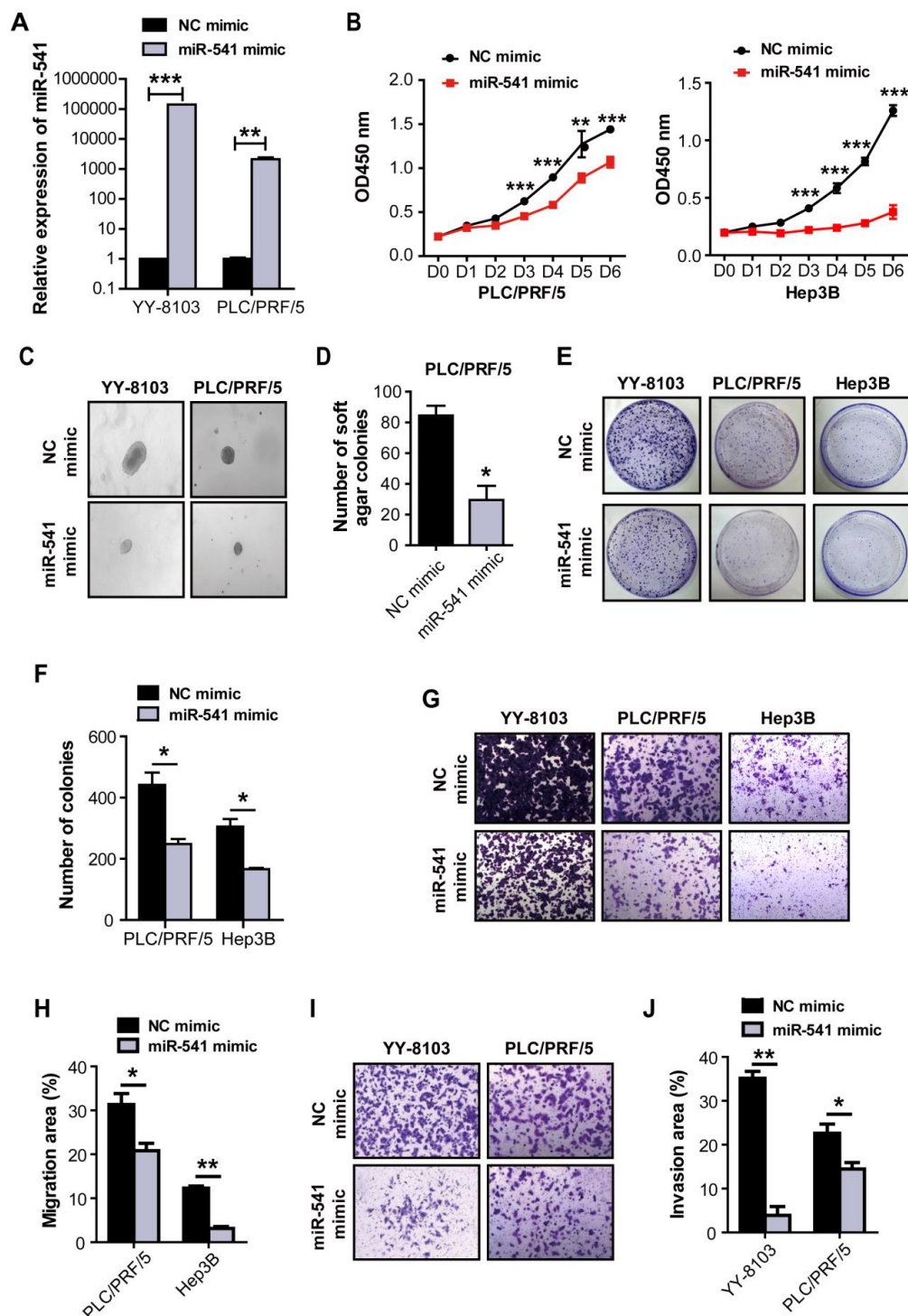


Figure S3. miR-541 suppresses the proliferation, colony formation, migration and invasion of HCC cells.

(A) Transfection of miR-541 mimic significantly increased the expression of miR-541 in

HCC cells. ** $P < 0.01$ and *** $P < 0.001$ by two-tailed Student's t-test. (B) Transfection of miR-541 mimic inhibited the proliferation of PLC/PRF/5 (left) and Hep3B (right) cells. ** $P < 0.01$ and *** $P < 0.001$ by two-tailed Student's t-test. (C) Representative images of the soft agar colony formation assays performed in YY-8103 (left) and PLC/PRF/5 (right) cells transfected with miR-541 mimic or negative control (NC) mimic. (D) miR-541 mimic inhibited the soft agar colonies in PCL/PRF/5 cells. * $P < 0.05$ by two-tailed Student's t-test. (E) Representative images of colony formation assays performed in YY-8103 (left), PLC/PRF/5 (middle) and Hep3B (right) cells transfected with miR-541 mimic or NC mimic. (F) miR-541 mimic suppressed the colony-formation ability of PLC/PRF/5 and Hep3B cells. * $P < 0.05$ by two-tailed Student's t-test. (G) Representative images of the migration assays performed in YY-8103 (left), PLC/PRF/5 (middle) and Hep3B (right) cells transfected with miR-541 mimic or NC mimic. (H) miR-541 mimic inhibited the migration of PCL/PRF/5 and Hep3B cells. * $P < 0.05$ and ** $P < 0.01$ by two-tailed Student's t-test. (I) Representative images of the invasion assays performed in YY-8103 (left) and PLC/PRF/5 (right) cells transfected with miR-541 mimic or NC mimic. (J) miR-541 mimic suppressed the invasion of YY-8103 and PLC/PRF/5 cells. * $P < 0.05$ and ** $P < 0.01$ by two-tailed Student's t-test. Above experiments were performed in triplicate and data are represented as means \pm SD.

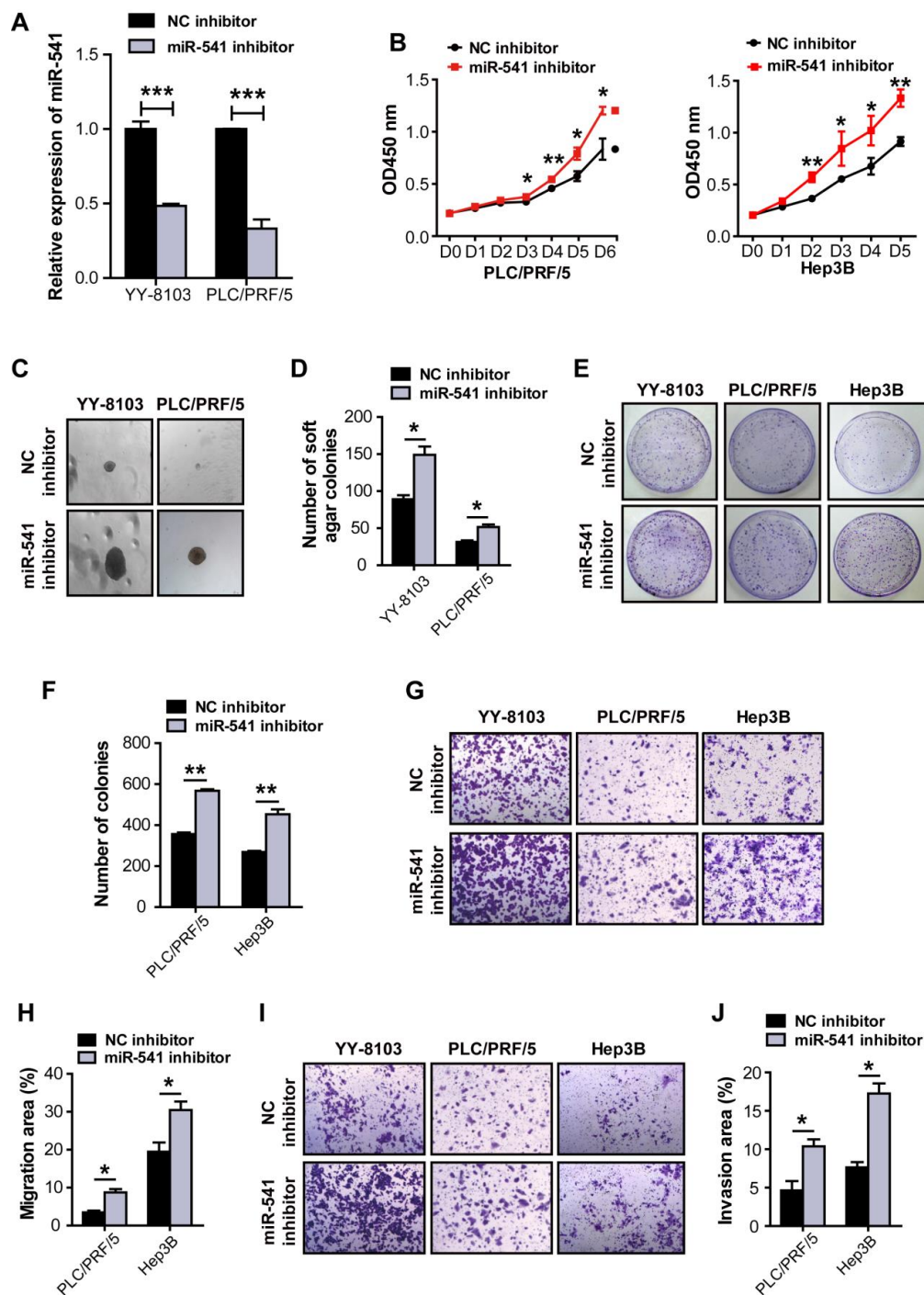


Figure S4. Inhibition of miR-541 promotes proliferation, colony formation, migration and invasion of HCC cells.

(A) Transfection of miR-541 inhibitor significantly reduced the expression of miR-541 in

HCC cells. *** $P < 0.001$ by two-tailed Student's t-test. (B) Transfection of miR-541 inhibitor enhanced the proliferation of PLC/PRF/5 (left) and Hep3B (right) cells. * $P < 0.05$ and ** $P < 0.01$ by two-tailed Student's t-test. (C) Representative images of the soft agar colony formation assays performed in YY-8103 (left) and PLC/PRF/5 (right) cells transfected with miR-541 inhibitor or negative control (NC) inhibitor. (D) miR-541 inhibitor promoted the soft agar colonies in PCL/PRF/5 cells. * $P < 0.05$ by two-tailed Student's t-test. (E) Representative images of the colony formation assays performed in YY-8103 (left), PLC/PRF/5 (middle) and Hep3B (right) cells transfected with miR-541 inhibitor or NC inhibitor. (F) miR-541 inhibitor augmented the colony-formation ability of PLC/PRF/5 and Hep3B cells. ** $P < 0.01$ by two-tailed Student's t-test. (G) Representative images of the migration assays performed in YY-8103 (left), PLC/PRF/5 (middle) and Hep3B (right) cells transfected with miR-541 inhibitor or NC inhibitor. (H) miR-541 inhibitor enhanced the migration of PCL/PRF/5 and Hep3B cells. * $P < 0.05$ by two-tailed Student's t-test. (I) Representative images of the invasion assays performed in YY-8103 (left) and PLC/PRF/5 (middle) and Hep3B (right) cells transfected with miR-541 inhibitor or NC inhibitor. (J) miR-541 inhibitor promoted the invasion of PLC/PRF/5 and Hep3B cells. * $P < 0.05$ by two-tailed Student's t-test.

Above experiments were performed in triplicate and data are presented as means \pm SD.

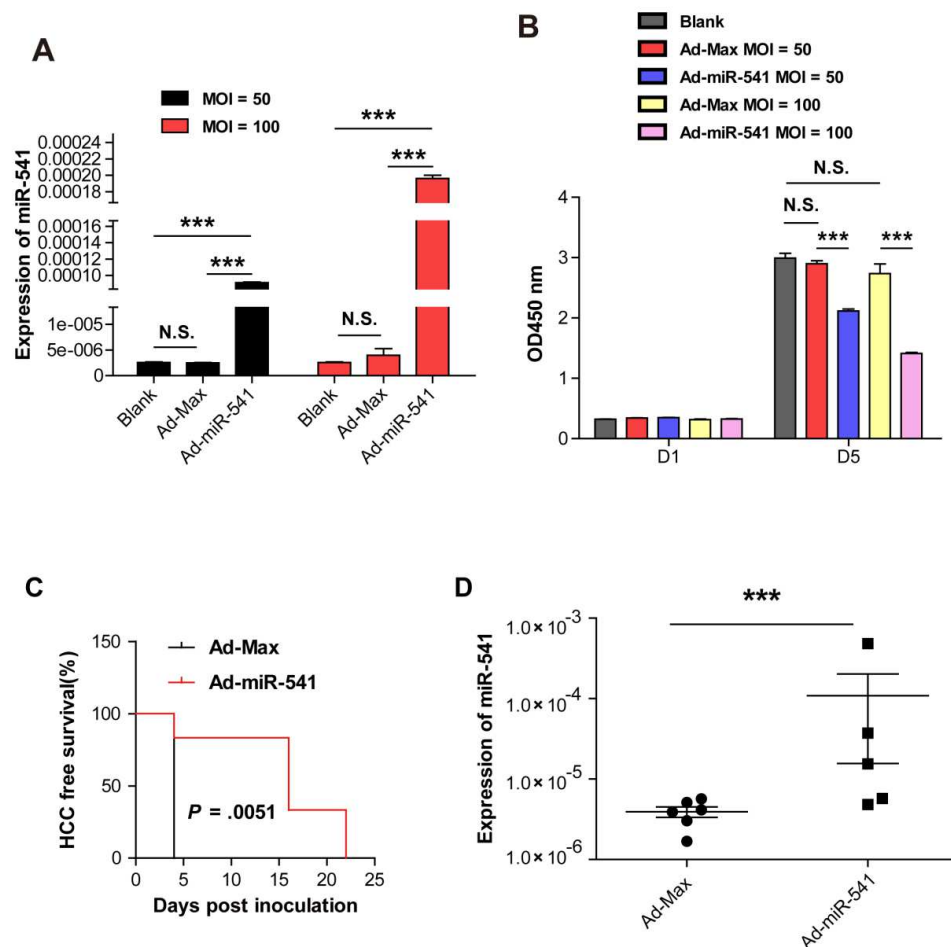


Figure S5. Ad-miR-541 inhibits growth of HCC cells.

(A) Adenovirus expressing miR-541 increased the expression of miR-541 in a dose-dependent manner. (B) Adenovirus-mediated overexpression of miR-541 inhibits proliferation of HCC cells in a dose-dependent manner. (A and B) * $P < 0.05$, ** $P < 0.01$, *** $P < 0.001$ by two-tailed Student's t-test. (C) HCC-free survival curve of xenografts in the mice receiving cells infected with adenovirus expressing miR-541 (Ad-miR-541) or in the mice receiving cells infected with control virus Ad-Max at a MOI of 100. $n = 6$ in each group. $P = 0.0051$, log-rank test. (D) Expression of miR-541 in the xenografts from mice

receiving cells infected with Ad-miR-541 or Ad-Max at a MOI of 100. n = 6 in each group.

*** $P < 0.001$ by Wilcoxon's matched pairs test.

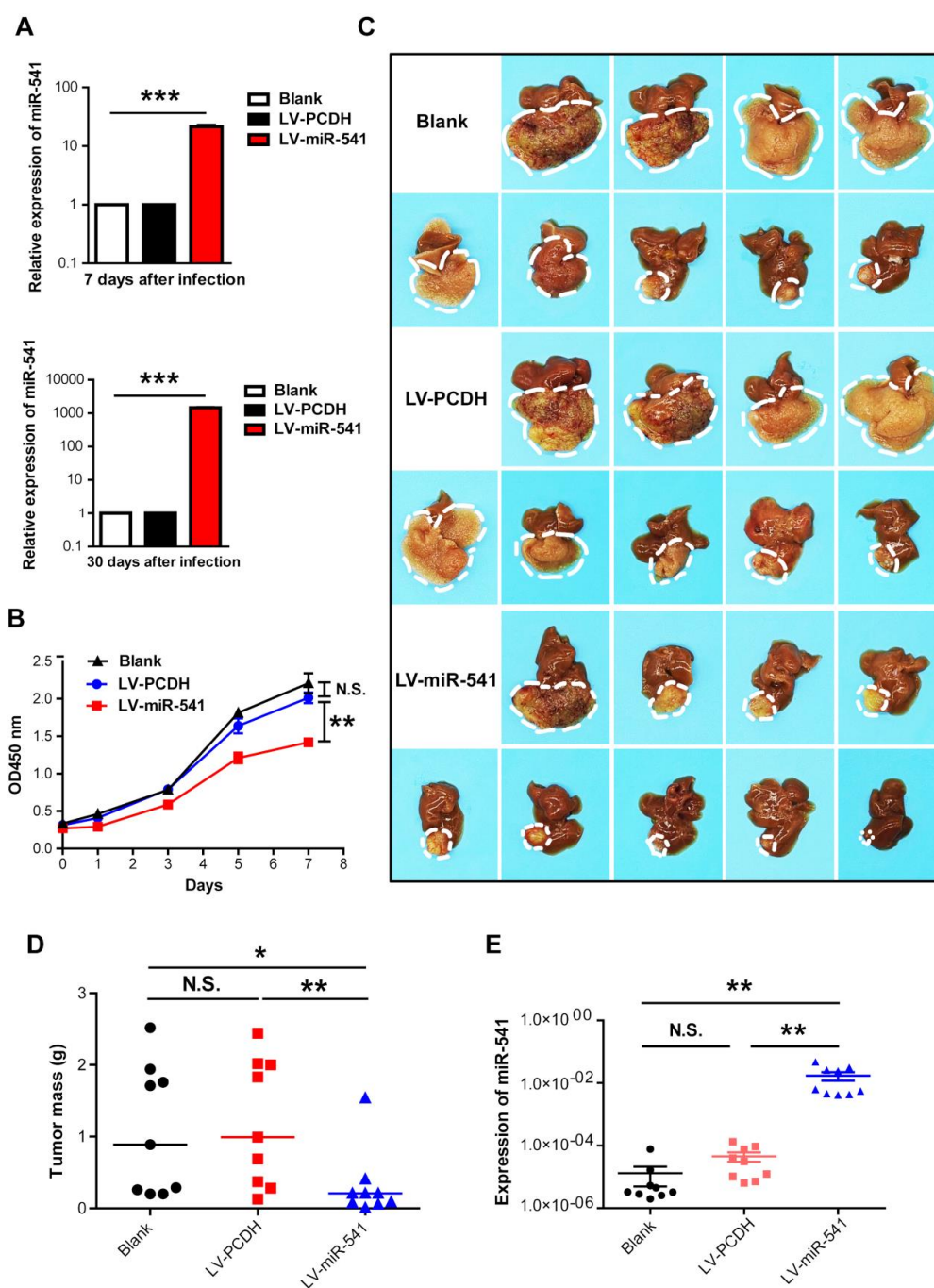


Figure S6. Lentivirus-mediated miR-541 overexpression suppresses the growth of orthotopically-implanted HCC tumors.

(A) YY-8103 cells were infected with Lentivirus expressing miR-541 (LV-miR-541) and control virus (LV-PCDH). The expression of miR-541 was detected by real-time PCR at 7 days (the top) and 30 days (the bottom) after infection. (B) LV-miR-541 inhibited the proliferation of YY-8103 cells. (A and B) ** $P < 0.01$, *** $P < 0.001$ by two-tailed Student's t-test. (C) The images of tumor nodules from orthotopic HCC models established with YY-8103 cells infected with LV-miR-541 or the control virus (LV-PCDH) and YY-8103 cells without lentivirus treatment (Blank) White dotted lines denote the boundary of tumors. (D) Statistical analysis of tumor weights in different groups. (E) Real-time PCR analysis was used to detect the expression of miR-541 in tumor nodules of these three groups. (D and E) $n = 9$ in each group. * $P < 0.05$, ** $P < 0.01$ by Mann-Whitney test.

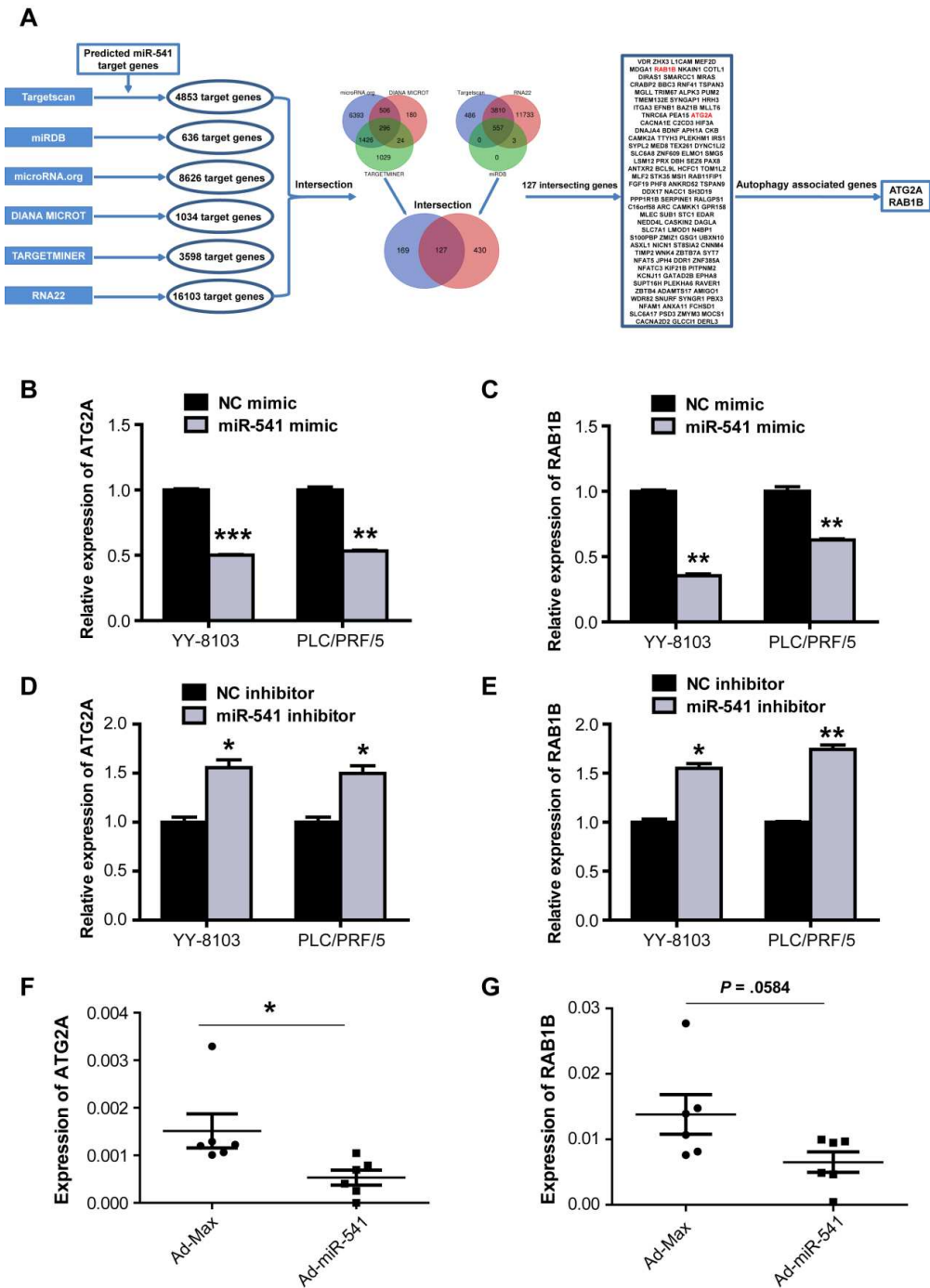


Figure S7. miR-541 reduces expression of ATG2A and RAB1B *in vitro* and *in vivo*.

(A) The potential target genes of miR-541 were searched in six commonly-used miRNA prediction programs, and an intersection of the resultant target genes were performed. This

approach identified 127 intersecting genes, and ATG2A and RAB1B were the only two autophagy associated genes among these intersecting genes. (B and C) miR-541 mimic reduced expression of ATG2A (B) and RAB1B (C) mRNA in HCC cells. (D and E) Expression of ATG2A (D) and RAB1B (E) in HCC cells transfected with miR-541 inhibitor or negative control (NC). (B-E) * $P < 0.05$, ** $P < 0.01$ and *** $P < 0.001$ by two-tailed Student's t-test. Above experiments were performed in triplicate and data are shown as mean \pm SD. (F and G) Expression of ATG2A (F) and RAB1B (G) mRNA in xenografts from mice receiving injection of YY-8103 cells infected with Ad-Max or Ad-miR-541. $n = 6$ in each group. * $P < 0.05$ by Wilcoxon's matched pairs test.

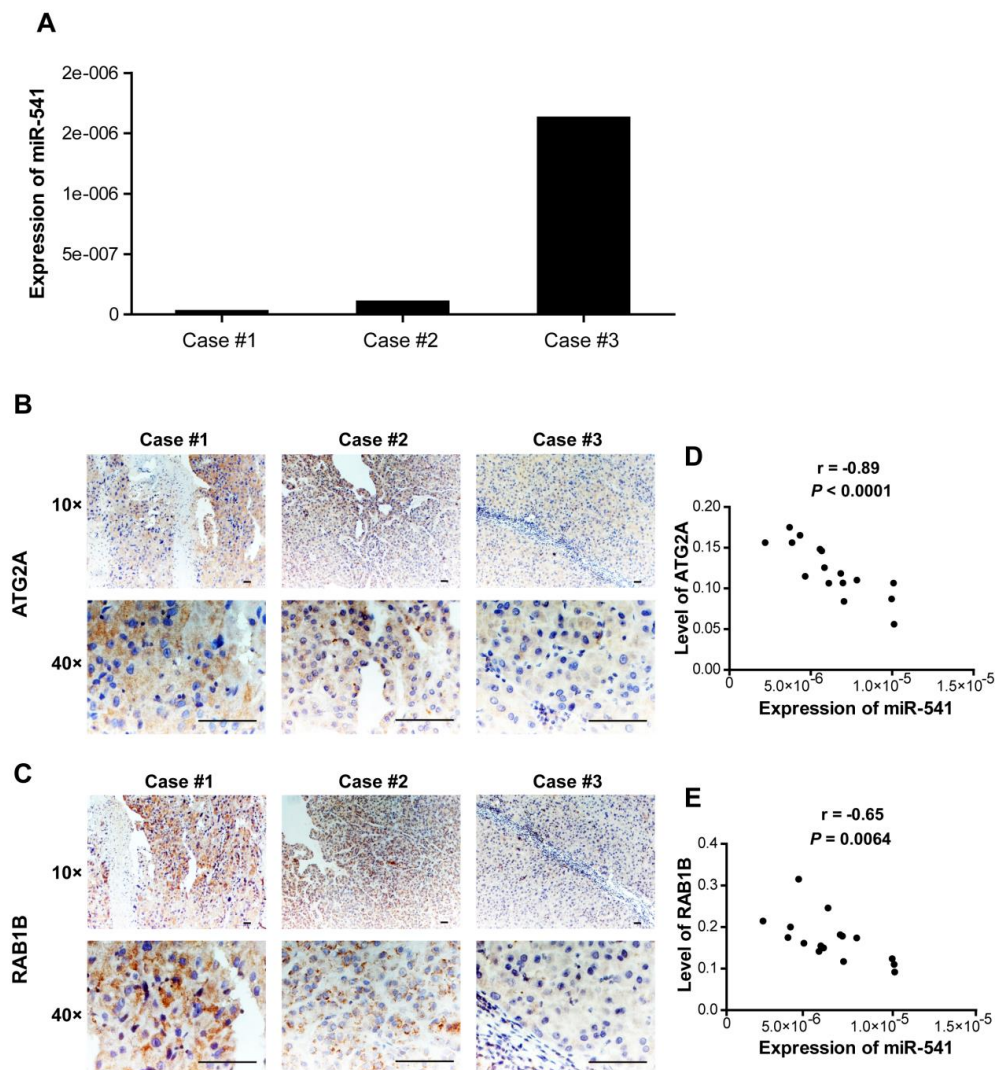


Figure S8. Immunohistochemical (IHC) staining of ATG2A and RAB1B in human HCC tissues with different levels of miR-541.

(A) Real-time PCR analysis of miR-541 expression in the case #1, case #2 and case #3 patients. (B and C) IH analyses showed that HCC samples with higher miR-541 level displayed less ATG2A (B) and RAB1B (C) expression and vice versa. (D and E) miR-541 expression was negatively correlated to the levels of ATG2A (D) and RAB1B (E). Scale bar, 100 μ m. The values of r represent spearman's correlation coefficients.

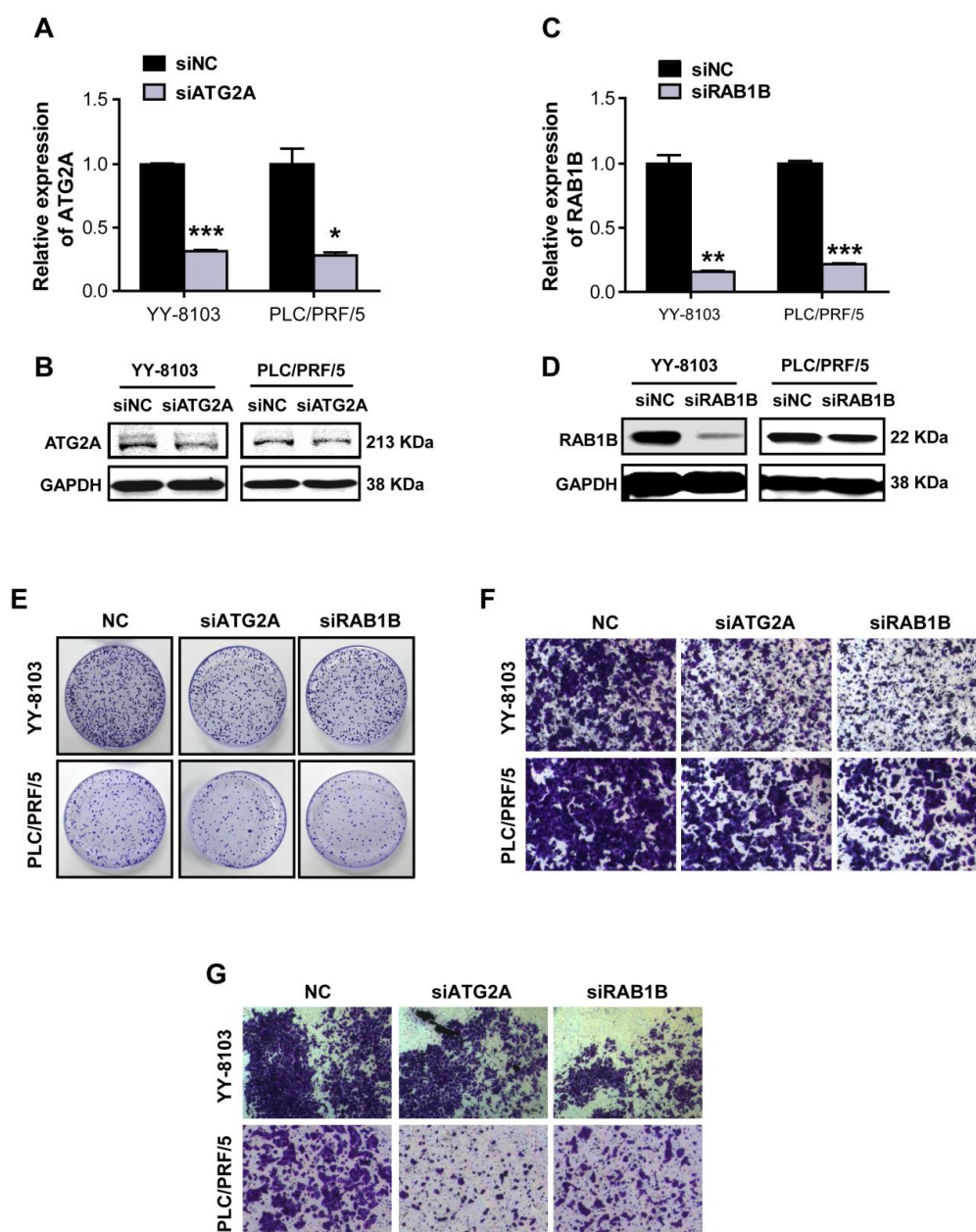


Figure S9. siRNA targeting ATG2A and RAB1B inhibits the colony formation, migration and invasion of HCC cells.

(A and B) Expression of ATG2A mRNA (A) and protein (B) in HCC cells transfected with siRNA targeting ATG2A (siATG2A) and negative control (siNC). (C and D) siRNA targeting RAB1B inhibited expression of RAB1B mRNA (C) and protein (D). (A and C) * $P < 0.05$, **

$P < 0.01$ and *** $P < 0.001$ by two-tailed Student's t-test. (E) Representative images of the colony-formation assays in YY-8103 cells and PLC/PRF/5 cells transfected with siNC, siATG2A and siRAB1B. (F) Representative images of the migration assays in YY-8103 cells and PLC/PRF/5 cells transfected with siNC, siATG2A and siRAB1B. (G) siATG2A and siRAB1B inhibited the invasion of YY-8103 cells and PLC/PRF/5 cells.

Above experiments were performed in triplicate and data are presented as means \pm SD.

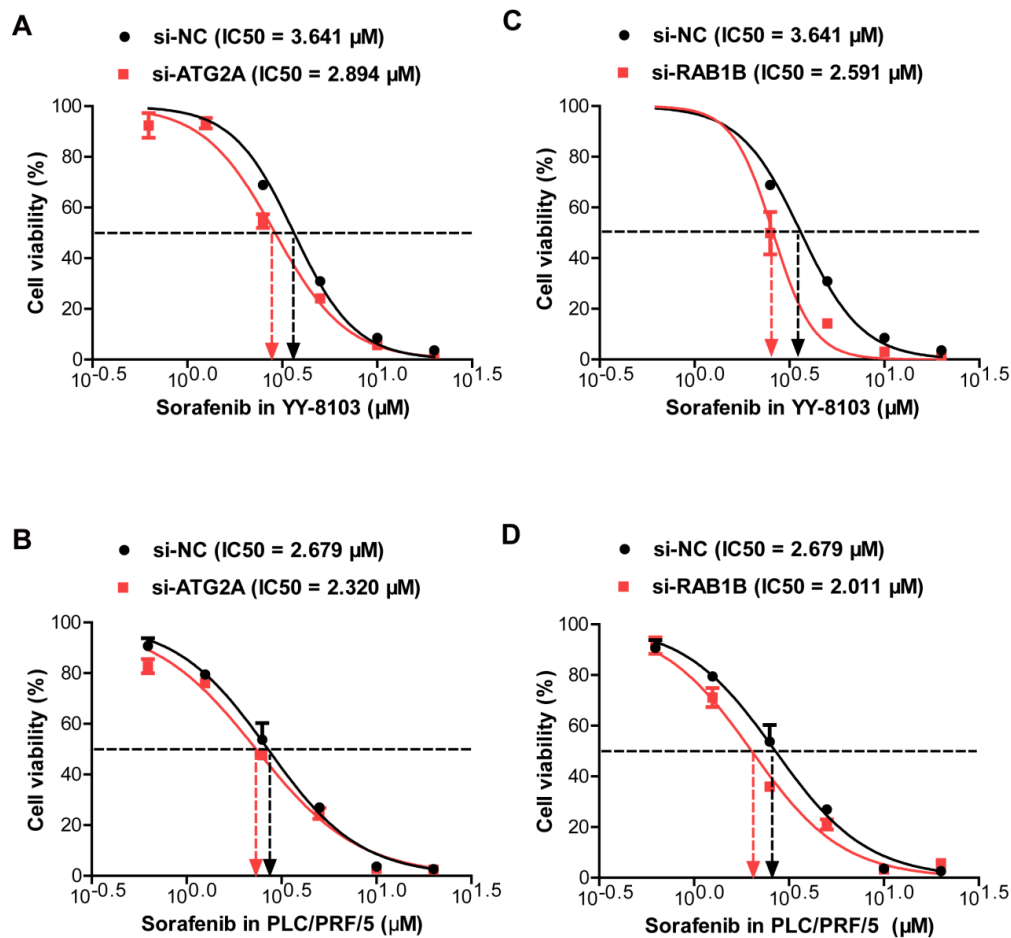


Figure S10. Downregulation of ATG2A and RAB1B enhances the sensitivity of HCC cells to sorafenib.

(A and B) Dose-response curves of YY-8103 cells (A) and PLC/PRF/5 cells (B) transfected with the siRNA targeting ATG2A (si-ATG2A) or negative control (si-NC) and treated with sorafenib. (C and D) Dose-response curves of YY-8103 cells (C) and PLC/PRF/5 cells (D) transfected with the siRNA targeting RAB1B (si-RAB1B) or negative control (si-NC) and treated with sorafenib. Bars denote the SD, with $n = 3$ for each treatment combination.

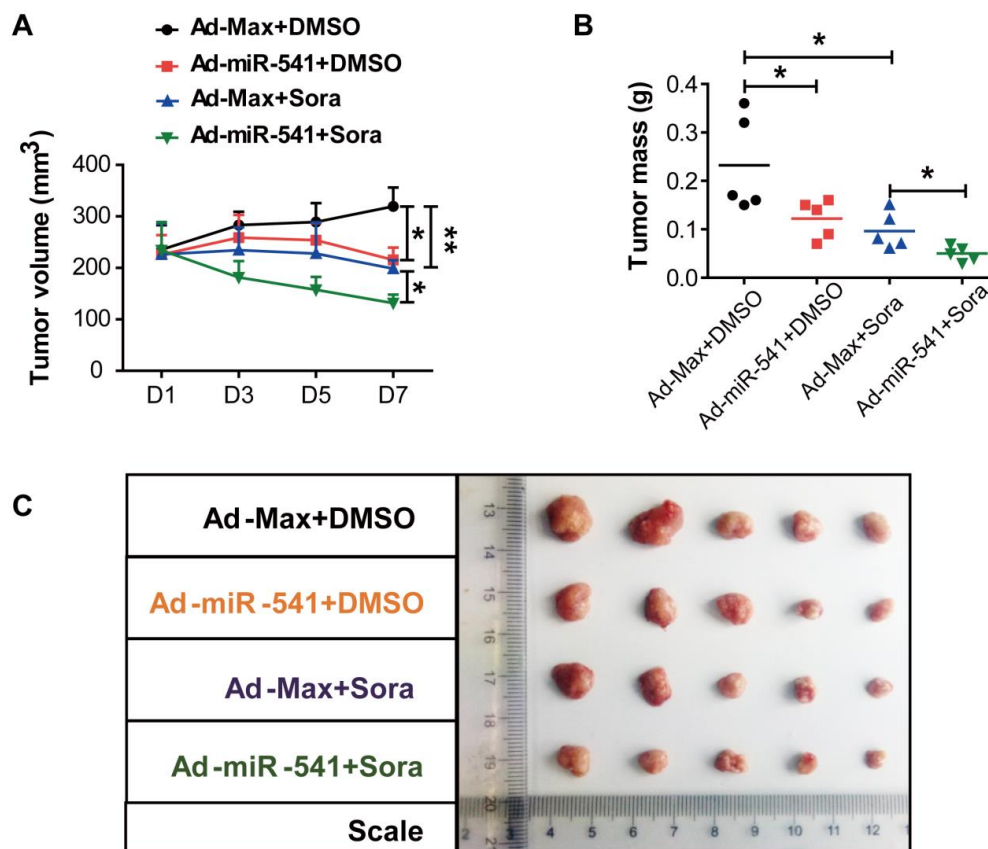


Figure S11. miR-541 enhances suppressive effects of sorafenib on the growth of HCC cells *in vivo*.

(A) Mice with PLC/PRF/5 cells-derived xenografts were received intratumoral injections with Ad-miR-541 or Ad-Max combined with intraperitoneal treatments with sorafenib or vehicle DMSO. The volumes of xenografts were detected and compared between indicated groups. $n = 5$ in each group, * $P < 0.05$, ** $P < 0.01$ by nonparametric Mann-Whitney test. (B) Statistical analysis of tumor weights in different groups, $n = 5$ in each group, * $P < 0.05$ by nonparametric Mann-Whitney test. (C) Representative images of xenografts in the indicated groups.

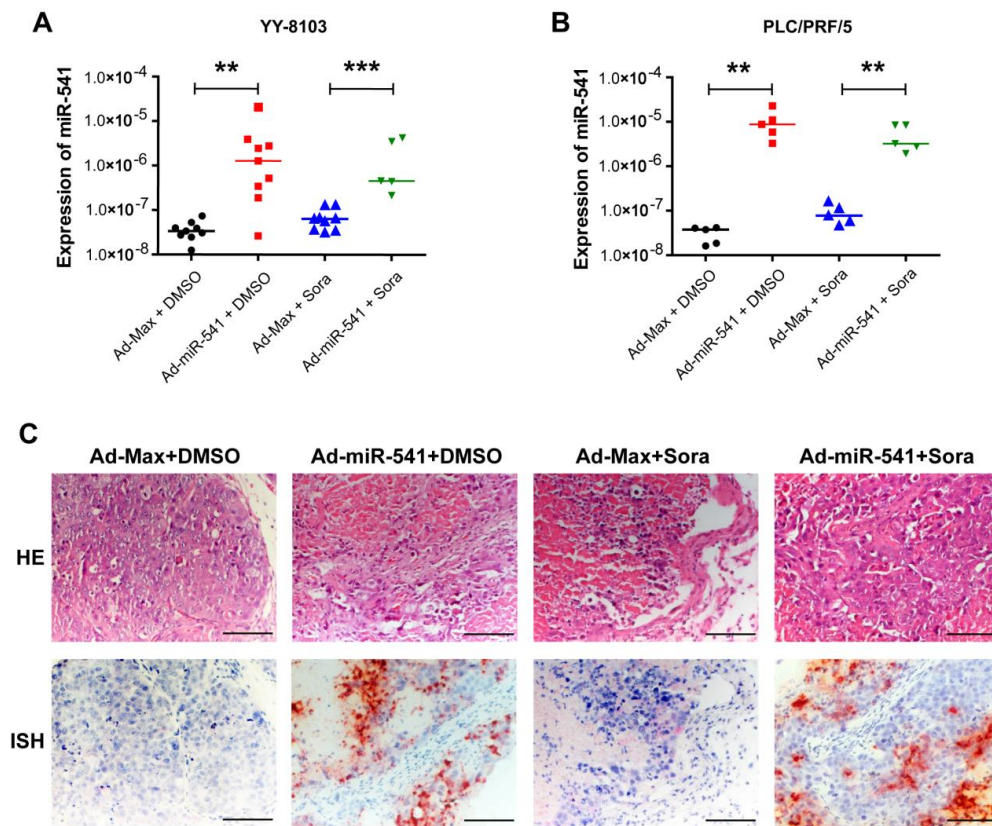


Figure S12. The expression of miR-541 in xenografts treated with Ad-miR-541 and sorafenib.

(A and B) Expression of miR-541 in YY-8103 (A) or PLC/PRF/5 (B) xenografts that received intratumor injections of Ad-miR-541 or Ad-Max combined with intraperitoneal injections of sorafenib or the DMSO vehicle. ** $P < 0.01$ and *** $P < 0.001$ by Mann-Whitney test. (C) H&E (HE) staining and in situ hybridization (ISH) analysis of miR-541 expression in PLC/PRF/5 xenografts.

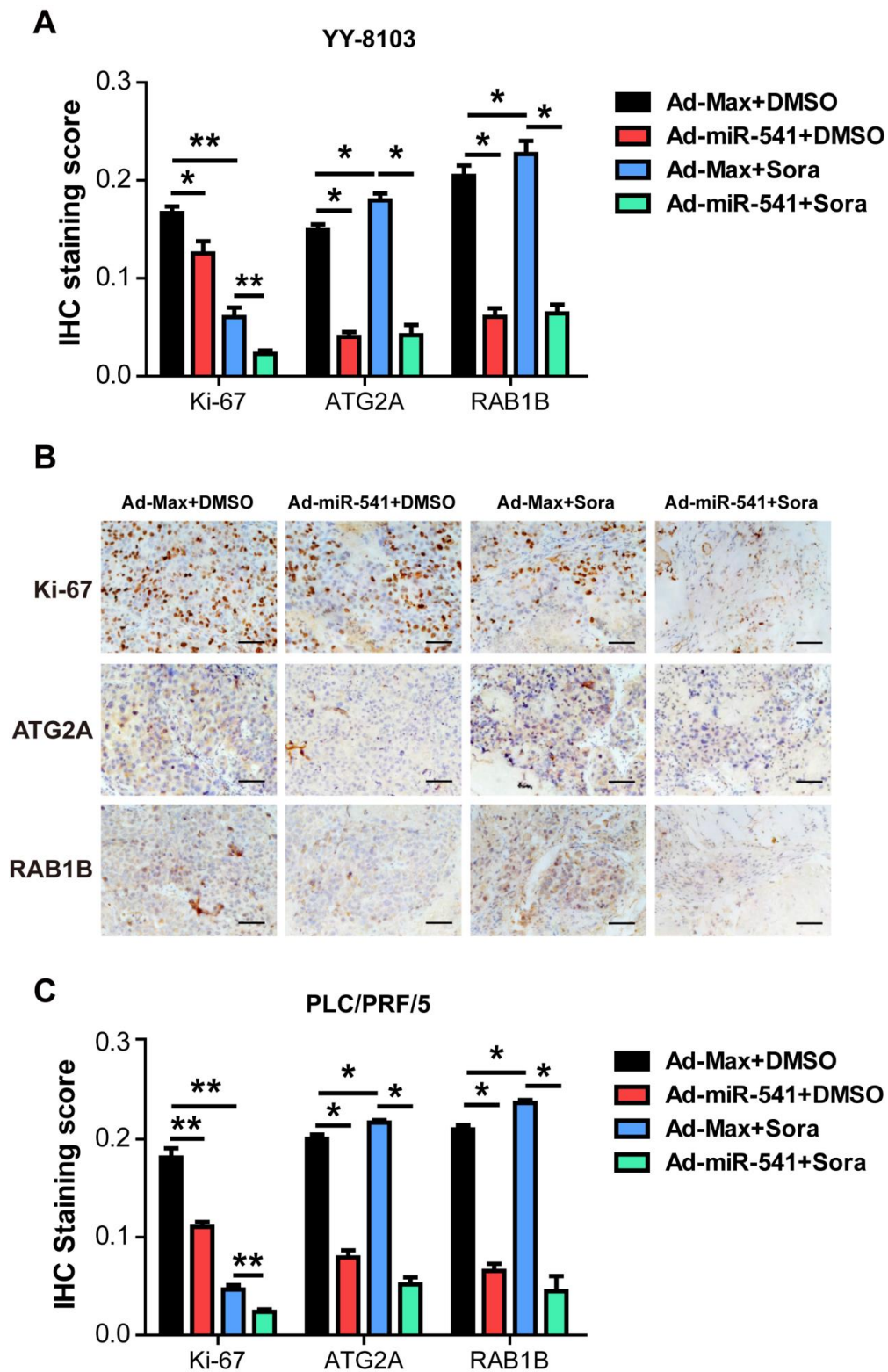


Figure S13. Ad-miR-541 injection downregulates the levels of Ki-67, ATG2A and RAB1B in the subcutaneously transplanted mice HCC model.

(A) Statistical analysis of immunohistochemical (IHC) scores of Ki-67, ATG2A and RAB1B staining in YY-8103 xenografts that received intratumor injections of Ad-miR-541 or Ad-Max combined with intraperitoneal injections of sorafenib or the DMSO vehicle. * $P < 0.05$, ** $P < 0.01$ by Mann-Whitney test. (B) IHC staining for Ki-67, ATG2A and RAB1B in PLC/PRF/5 xenografts treated with Ad-miR-541 and sorafenib. Scale bar, 100 μm . (C) Statistical analysis of IHC scores of Ki-67, ATG2A and RAB1B staining in PLC/PRF/5 xenografts. (A and C) * $P < 0.05$ and ** $P < 0.01$ by Mann-Whitney test.

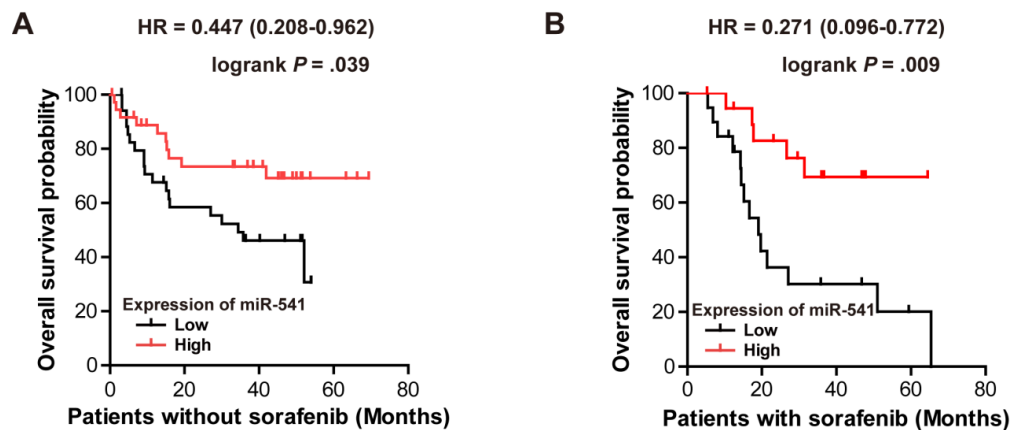


Figure S14. Overall survival (OS) of patients with low and high miR-541 expression in sorafenib-treated group and sorafenib-untreated group, respectively.

The Kaplan-Meier analysis was used to compare OS for patients with low and high miR-541 expression in orafenib-untreated group (A) and sorafenib-treated group (B), respectively.

Log-rank test was used to calculate the P values and cox-regression analysis was used to calculate the hazard ratio (HR) in the indicated analysis.

Supplementary Table 1. Sequences of primers used in Real-time PCR

Sequences (5'-3')	
Human β -actin forward	CATCCTGCGTCTGGACCT
Human β -actin reverse	GTACTTGCGCTCAGGAGGAG
Human ATG2A forward	CACTGCGGTTGCACAAAG
Human ATG2A reverse	GTACAAGGCGGAGTCATCG
Human RAB1B forward	CCGCCATGAACCCCGAATATGAC
Human RAB1B reverse	GGGACATCATCTGGAGAAGGTGC

Supplementary Table 2. Sequences of oligonucleotides in this study

Oligonucleotides	Sequences (5'-3')
hsa-miR-541-3p mimic	UGGUGGGCACAGAAUCUGGACU
Negative control for miRNA mimic (NC mimic)	UUGUACUACACAAAAGUACUG
hsa-miR-541-3p inhibitor	AGUCCAGAUUCUGUGCCCACCA
Negative control for miRNA inhibitor (NC inhibitor)	CAGUACUUUUGUGUAGUACAA
siATG2A sense	GCUACUUGCUGCACCAUATT
siATG2A antisense	UAGUGGUGCAGCAAGUAGCTT
siRAB1B sense	CGUACACAGAGAGCUACAUTT
siRAB1B antisense	AUGUAGCUCUCUGUGUACGTT
Negative control for siRNA (siNC) sense	UUCUUCGAACGUGUCACGUTT
Negative control for siRNA (siNC) antisense	ACGUGACACGUUCGGAGAATT

Supplementary Table 3. Sequences of primers used for sub-cloning and plasmid construction

Sequences (5'-3')				
psicheck2-ATG2A	3'UTR	Wild	CCGCTCGAGTCAAGTGGCGCTCGGACAGT	
type forward				
psicheck2-ATG2A	3'UTR	Wild	ATAAGAATGCGGCCGCTGGCGGTGGGCAGTTTATTC	
type reverse				
psicheck2- RAB1B	3'UTR	Wild	CCGCTCGAGACAGCACCCCTGTAAAGCCG	
type forward				
psicheck2- RAB1B	3'UTR	Wild	ATAAGAATGCGGCCGCTCCATCTTTCCCCAAGTGGC	
type reverse			CCGGAATTCGCCACCGTGACCAGCATTGCACATGGC	
pDC315-miR-541-EcoRI forward			TTTC	
pDC315-miR-541-NheI reverse			CTAGCTAGCTGACCCTGTAGGGACCCCTGCACAAG	

Supplementary Table 4. miR-541 expression correlates with aggressive phenotypes.

Variables	miR-541			<i>p</i> Value*
	All cases (n=120)	Low expression (n=72)	High expression (n=48)	
Age (years)				
≤ 55†	61	37	24	0.881
> 55	59	35	24	
Sex				
Male	108	66	42	0.456
Female	12	6	6	
HBsAg				
Absent	22	11	11	0.289
Present	98	61	37	
Liver cirrhosis				
No	19	12	7	0.759
Yes	101	60	41	
AFP (ng/ml)				
≤ 20	44	27	17	0.817
> 20	76	45	31	
Differentiation				
I - II	17	14	3	0.042
III-IV	103	58	45	
Tumor size (cm)				
≤ 10	87	47	40	0.030
> 10	33	25	8	
Tumor staging				
TNM I	42	18	24	0.035
TNM II	31	23	8	
TNM III	43	28	15	
TNM IV	4	3	1	
Microvascular invasion				
Absent	51	26	25	0.083
Present	69	46	23	
Tumor microsatellite				
Absent	55	34	21	0.708
Present	65	38	27	
Tumor encapsulation				
Incomplete or absent	87	57	30	0.045
Present and intact	33	15	18	

* χ^2 test. † Median age. The cut-off point for separating HCCs with high expression of miR-541 with low level of miR-541 was 1. HBsAg, hepatitis B surface antigen; AFP, α -fetoprotein.

Reference

1. Liu J, Chen S, Wang W, et al. Cancer-associated fibroblasts promote hepatocellular carcinoma metastasis through chemokine-activated hedgehog and TGF- β pathways. *Cancer Lett.* 2016;379:49-59.